UNIFIED NLTE MODEL ATMOSPHERES INCLUDING SPHERICAL EXTENSION AND STELLAR WINDS

RUDOLF GABLER, ASTRID GABLER, ROLF-PETER KUDRITZKI, JOACHIM PULS, ADALBERT PAULDRACH
Universitätssternwarte München, Scheinerstr.1,
8000 München 80

ABSTRACT We present NLTE model atmospheres for hot stars that avoid the artificial division between hydrostatic photosphere and supersonic stellar wind envelope. The models are of spherical geometry and extended over the entire sub- and supersonic atmosphere. They need only stellar effective temperature, gravity and radius – defined at the inner atmospheric boundary – as free parameters and are in principle selfconsistent. The models yield stellar energy distributions and hydrogen and helium line spectra. First calculations for the O4f star ζ Puppis are presented. The main result are:

1. Our new kind of modeling stellar atmospheres can reproduce "photospheric" lines (which are "wind contaminated" in some cases) as well as typical "wind" lines.
2. The observed infrared excess of ζ Puppis is reproduced by the unified model (can't be done with hydrostatic models).
3. The emergent flux shortward of the HeII-edge at 228 Å is increased by a factor of thousand relative to plane-parallel models. This is caused by the presence of the wind outflow in the region where the continuum is formed. This effect plays an important role for the ionization of surrounding interstellar gas and might be a very promising way to solve the long-standing problem of the "Zanstra discrepancy" for Central Stars.

INTRODUCTION

The present treatment of atmospheres of hot stars divide artificially between photospheric layers and supersonic stellar wind envelopes. This has several important consequences :

1. The location of the borderline between these two regions has to be defined as a free parameter. Normally either a "photospheric outflow velocity" v_o is adopted, that fixes the density ρ_o at this boundary via the equation of continuity, or the radius of the sonic point r_s is fixed from an ad hoc velocity law that again

yields ρ_o in the same way. As test calculations not only for H_α and He II 4686 but also for the near and far infrared continuum show, this free parameter strongly influences the amount of (central) line emission and IR continuum shape.

2. The radiative interaction between photosphere and winds needs to be specified. Normally, the emergent flux of the plane-parallel NLTE models without winds is taken as the inner radiative boundary of the wind region. Apart from the important effect of wind blanketing for the photospheres (see Abbott and Hummer, 1985) this procedure is most probably correct for the continous radiation field of O stars between 228 Å and 10000 Å. However, shortward of 228 Å (the He II -edge) the continuum becomes optically thick only far out in the stellar wind. This has crucial consequences for the He II line formation problem and the line formation of ions with ionization edges in that spectral region (Pauldrach, 1987a, b; Pauldrach and Herrero, 1988). Simple "on the spot" or "escape probability" approximations for the formation of this continuum lead to spurious results compared with the solution of the exact radiative transfer problem of this case.

3. Line cores are also not optically thin at this artificial boundary between photosphere and wind. Thus, the normal procedure of taking the line profiles of the photospheric NLTE models as inner boundary condition for the wind radiative transfer or, even worse, just simply adding them to the wind emission or ignoring the photospheric line radiation completely, is consequently questionable.

4. To investigate if the "classical" NLTE analysis lines like H_γ, H_β, He II 4542, 5412 are "wind contaminated" or not, is impossible with a artificial division of the atmosphere.

5. Last but not least, from a purely theoretical standpoint the introduction of additional free parameters is unsatisfactory.

We conclude therefore that "Unified" model atmospheres are needed, which treat both the photosphere and the supersonic stellar wind region and present in this paper a first step towards the development of such a theory.

METHOD

The principle input parameters for our model are specified at a fixed Thomson optical depth ($\tau_{Th} \approx 50$) in the atmosphere:

$$T^*_{eff},\ g^*,\ R^*$$

The value of τ_{Th} is large enough to assure that the continuous radiation is thermalized at all wavelengths at this depth. The corresponding Rosseland optical depth τ_{Ross} is than larger than 100 in all cases. For this set of parameter, the theory of radiation driven winds as recently extended by Pauldrach et al. (1986) yields force multiplier parameters k, α, δ which compose the force multiplier M:

$$M\left(\rho, v, \frac{dv}{dr}, r, n_e\right) = k\cdot\left(\frac{\sigma_e \rho v_{th}}{dv/dr}\right)^{-\alpha} \cdot \left(\frac{n_e}{10^{11}\,W}\right)^{\delta} \cdot CF\left(r, v, \frac{dv}{dr}\right) \quad (1)$$

W: dilution factor, CF: finite cone angel corr. factor

and which determine the wind structure — massloss rate $\dot{M}$, velocity and density fields v(r), ρ(r) — because $M \sim g^{1}_{Rad}$ ("radiative line acceleration"). The stellar wind code does not include the energy balance. Thus a prespecified temperature stratification T(r) must be chosen as input at this stage. Pauldrach et al. have shown that the resulting density and velocity structure does not depend on the detailed choice of T(r) as long as the force multiplier parameters are fixed. Thus, for simplicity, T(r) = T_{eff} is adopted in the region where $v(r)/v_{sound} \geq 0.1$ in this first step, where in deeper layers a grey solution is chosen.

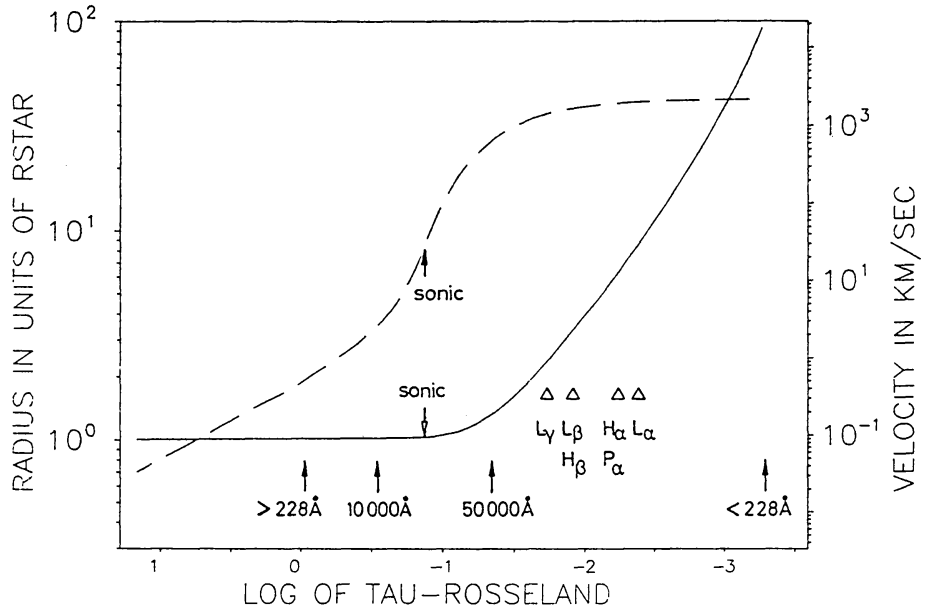

Fig. 1. Stellar radius r/R_* (fully drawn) and wind outflow velocity v (dashed) as a function of log τ_{Ross} for model B. The arrows indicate the sonic point and the depths where τ_ν=1 is reached for the corresponding wavelength. Triangles mark the depth where the cores of important lines become optically thin in the corresponding hydrostatic model.

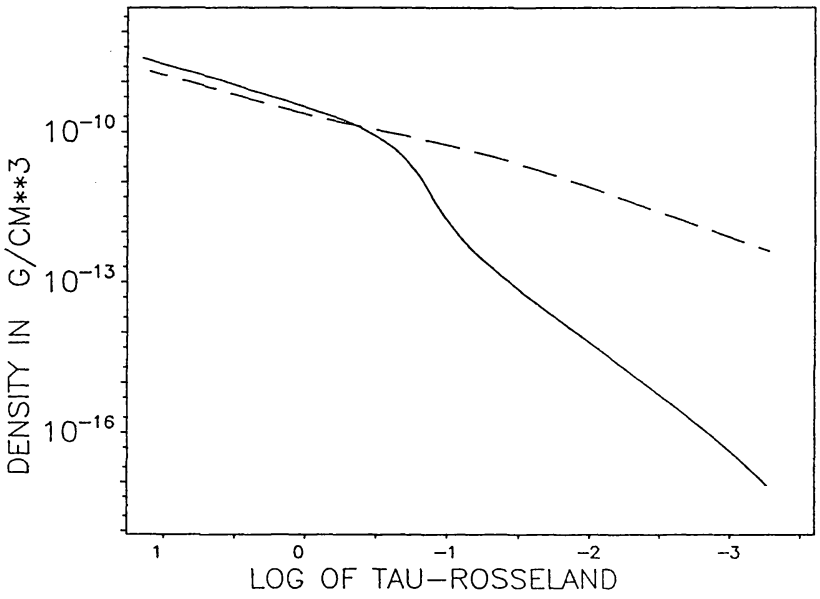

Fig. 2. Mass density ρ versus log τ_{Ross} for model B (fully drawn) and the corresponding plane-parallel hydrostatic model (dashed).

NLTE TEMPERATURE STRUCTURE

A NLTE model atmosphere code is written for spherically extended atmospheres (in principle similar to that of Mihalas and Hummer, 1974, except that the hydrostatic equation is removed and replaced by $\rho(r)$ computed from the stellar wind code). Opacities (bb in *Sobolev*, bf and ff plus Thomson scattering) are calculated for 5 H, 5 He I and 10 He II NLTE levels (and additional higher LTE levels) because these are the major opacity sources for hot stars and therefore direct comparison with standard plane-parallel NLTE models can easily be done.

The NLTE temperature is calculated from the constraint of *radiative equilibrium* :

$$\int_0^\infty \left(\chi_\nu J_\nu - \eta_\nu\right) d\nu = 0 \qquad \left.\begin{array}{l}\chi\text{: absorption}\\ \eta\text{: emission}\end{array}\right\} \text{coefficients} \qquad (2)$$

note It is not our intension to show whether in the whole atmosphere the radiative equilibrium constraint is fullfilled or not. But first, this approximation is probably good enough in the region we are interrested most — around the sonic point, where hydrogen and helium continua are formed— and second, to estimate the amount of energy dissipated nonradiatively it is necessary to adopt the simplest approximation (namely radiative equilibrium) and than proof how much energy dissipation is needed to fullfill the energy balance.

Another point is that the effects of NLTE metal opacity may be important for the temperature structure as many authors showed in the hydrostatic case (Mihalas, 1972, Husfeld et al., 1984, Anderson, 1985, Werner, 1988, Drew, 1988). Therefore the main future step in model calculation is, to include all the metal opacities in the computation of the radiative equilibrium, as it is already done in the hydrodynamic part of our unified models.

DETAILS OF THE SPHERICAL NLTE MODEL CODE

The "rate equations" are formulated including accelerated lambda iterarion (ALI) (see Werner and Husfeld, 1985) as recently coded by Pauldrach and Herrero (1988).

$$R_{ki} = 4\Pi \left(\frac{n_i}{n_k}\right)^* \int_{\nu_k}^{\infty} \frac{\sigma_{ik}}{h\nu} \frac{2h\nu^3}{c^2} \exp\left(-\frac{h\nu}{kT}\right) \Lambda^* \left(\frac{S_\nu^{l-2} - S_\nu^{l-1}}{S_\nu^{l-1}}\right) d\nu$$

$$+ 4\Pi \left(\frac{n_i}{n_k}\right)^* \int_{\nu_k}^{\infty} \frac{\sigma_{ik}}{h\nu} \left(J_\nu^{l-1} + \frac{2h\nu^3}{c^2}\right) \exp\left(-\frac{h\nu}{kT}\right) d\nu \qquad (3)$$

$$R_{ik} = 4\Pi \int_{\nu_k}^{\infty} \frac{\sigma_{ik}}{h\nu} J_\nu^{l-1} \, d\nu \qquad l: \text{ iteration}$$

The code allows to choose between :

— a *complete linearization* algorithm with fixed *Eddington factors* i.e. linearized are the equations of:

— transfer $\qquad \frac{\partial^2 (fqr^2 J)_\nu}{\partial \tau_\nu^2} = \frac{r^2}{q} (J_\nu - S_\nu)$

— charge-, particle conservation

— statistical equilibrium ("rate equation")

where in this part the vector of unknowns to be solved by a *Newton-Raphson* procedure is:

$$z = J_1,\ldots,J_{NF},T,n_e,n_p,n(H),n(He\ I),n(He\ II),n_{He\,III}$$

— and a "ALI" method with partially linearization, i.e the transfer equation is removed from the sample of linearized equations and the continuum radiation field is calculated only in a formal solution. Therefore the vector of unknowns in the *Newton-Raphson* procedure reduces to:

$$z = T,n_e,n_p,n(H),n(He\ I),n(He\ II),n_{He\,III}$$

After finishing the NLTE model atmosphere calculation, subsequent line radiation transfer in the *comoving frame* for the line profiles follow (cf. contribution of A.Gabler at this meeting).

RESULTS

TABLE I Models for the O4f star ζ Puppis

model	T_{eff}	log g	$R/R_\odot$	$\dot{M}(M_\odot/yr)$	v_∞(km/s)
A	42000 K	3.5	19.0	$4.4 \cdot 10^{-6}$	2042
B	45000 K	3.6	18.0	$5.9 \cdot 10^{-6}$	2196
	k=0.053	α=0.709	δ=0.052		

We employed two sets of models for this well observed bright object.

The first choice of parameters (model A) uses the results of Bohannan et al. (1986), based on new CCD observations of very high S/N. However, these parameters were obtained using plane-parallel hydrostatic NLTE models for the profile fit, including a simulation of the effect of wind blanketing.

We used for the figures shown below parameter set B, because we don't still account for this effect. As pointed out by Abbott and Hummer (1985) and Bohannan et al. it is necessary to increase T_{eff} and logg for models without wind blanketing.

NLTE temperature

Figure 3 displays the temperature stratifications. The dilution of the radiation field due to spherical extension in the unified model is the reason for the drop in temperature below that of the plane-parallel model between $0.0 > \log \tau_{Ross} > -1.0$ (see also Mihalas and Hummer, 1974; Gruschinske and Kudritzki, 1979).In the outer layers ($\log \tau_{Ross} \leq -2.5$) the hydrostatic model shows the typical temperature increase due to the overpopulation of the hydrogen ground state (Fig.4), which is caused by the onset of line cascading as soon as the hydrogen lines become optically thin.For layers with $\log \tau_{Ross} < -3.5$ (not plotted in Fig.3) the temperature drops again, which is due to the cooling by the He II ground state continuum, which becomes optically thin there in the hydrostatic model (see Auer and Mihalas, 1972 or Kudritzki, 1979). This temperature bump is also found in the unified models, however, at much larger Rosseland optical depth $\log \tau_{Ross} \approx -1.2$ .The reason for this is that due to the presence of the velocity field the lines start to desaturate close to the sonic point, so that line cascading becomes important already in these layers ($\log \tau_{Ross} \approx -0.8$). This explains the increase of temperature until $\log \tau_{Ross} \approx -1.2$. The temperature drop towards

lower optical depth is then again caused by cooling of the He II continuum which due to effects of the velocity field also becomes optically thin in much deeper layers.

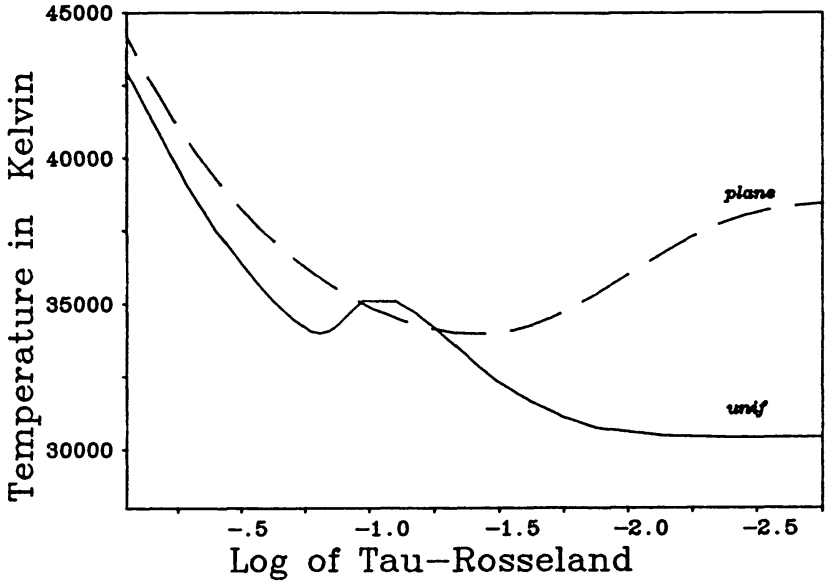

Fig. 3 Temperature versus $\log \tau_{Ross}$ for model B. The dashed curve represents a hydrostatic plane-parallel NLTE model (with only 6 hydrogen lines connecting the lower four levels and no helium lines), whereas the fully drawn curve belongs to the unified model including 10 hydrogen and 45 He II lines.

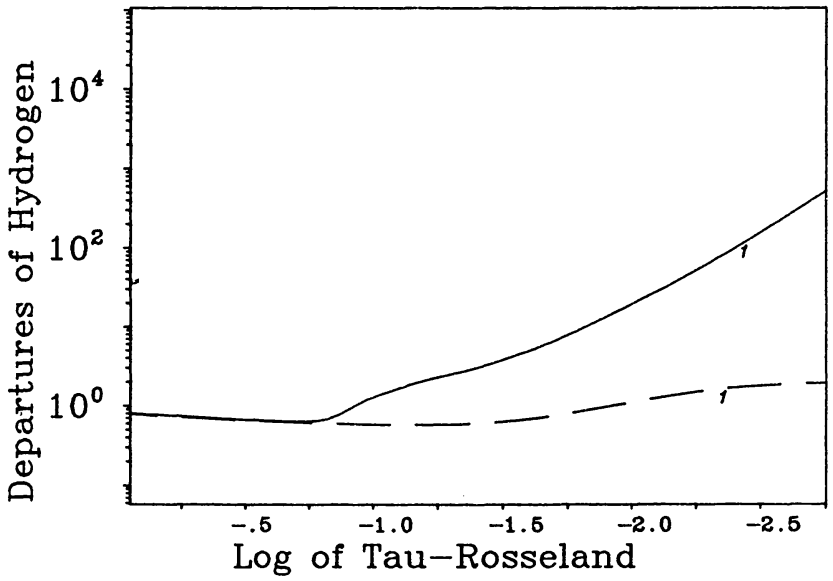

Fig. 4. Departure coefficient of the hydrogen ground level. Dashed: hydrostatic plane-parallel model, fully drawn: unified model.

He II groundstate

An important effect is seen in the He II ground state departure coefficient (Fig.5). In the hydrostatic model it increases strongly in the outer layers as soon as the continuum becomes optically thin. However, in the unified models (including the He II line transitions) we find a sharp drop in the He II ground state population between $0.3 \geq \tau_{Ross} \geq 0.01$. In a simple approach one can show, that a negative *line net radiative bracket* from level 1 to level 2:

$$Z_{21} = \beta \cdot \left(1 - \frac{W(r)}{r} \frac{I_c}{S_{12}} \right) \qquad (4)$$

$$\frac{I_c}{S_{12}} = \frac{b_1}{b_2} \cdot \exp\left(\frac{h\nu_{12}}{k} \left(\frac{1}{T_e} - \frac{1}{T_{Rad}} \right) \right) \qquad (5)$$

drives depopulation in the region of interrest (Fig.5). There we have

$$\frac{W(r)}{r} \frac{I_c}{S_{12}} > 1$$

because the dilution is not too large, and the radiation field which iluminates the line has a greater corresponding T_{Rad} than the local electrone temperature T_e (here: $T_{Rad} - T_e > 5000$ K). Further, for the small value of $\lambda_{12} = 303$ Å, even small temperature differences lead to a great effect.

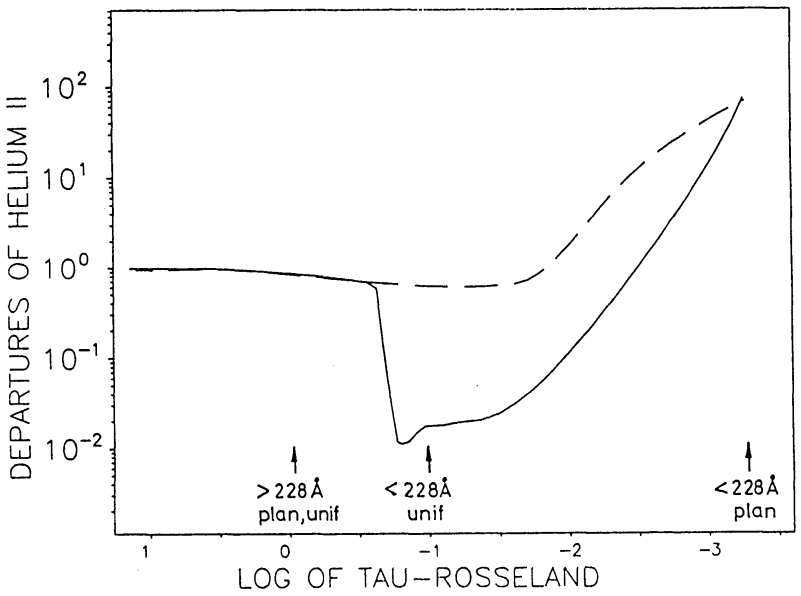

Fig. 5 Departure coefficient of the He II ground state as a function of $\log \tau_{Ross}$. Dashed: hydrostatic plane-parallel model, fully drawn: unified model. The arrows indicate $\tau_\nu = 1$ at the frequency of the continuum edge.

SPECTRA

The EUV to optical energy distribution is plotted in Fig.6. There are no observable effects present between 911 Å and 10 000 Å. This explains why hydrostatic plane-parallel NLTE models are able to fit the observed energy distribution in this spectral interval (see Kudritzki et al., 1983, Abbott and Hummer, 1985). The region between 911 Å and 228 Å is slightly affected. Here, the unified model produces a little flatter spectrum, that means appears a little cooler. However, shortward of 228 Å the emergent flux in the unified model is greatly enhanced. This is a simple consequence of the depopulation of the He II ground state as described in the foregoing paragraph. For the ionization of the surrouding gas, as for instance in H II regions or planetary nebulae, this effect will be important.

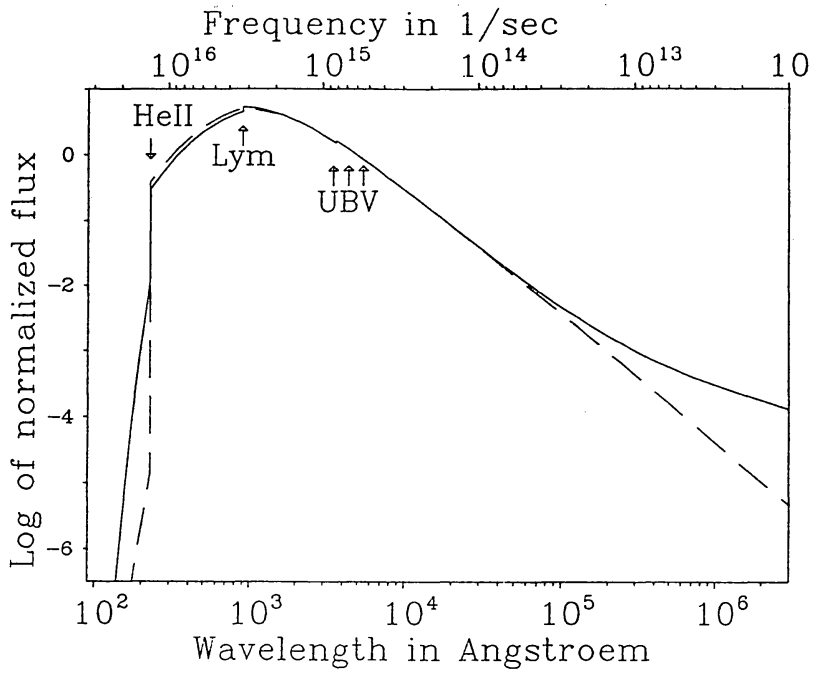

Fig. 6. EUV to visual energy distribution (fully drawn) and plane-parallel models (dashed). The He II-edge, the Lyman edge and the Johnson *U.B.V* bands are indicated.

Figure 7 compares the infrared flux predicted by the different models. While the hydrostatic plane-parallel models show the *Rayleigh-Jeans* tail of the energy distribution and fail to reproduce the observations, the unified models exhibit the expected IR-excess and come much closer to the observations. This is done by enhanced free-free emission of the extended wind envelope, as has been discussed by Panagia and Felli (1975), Wright and Barlow (1975), Castor and Simon (1983), and Lamers and Waters (1984).

note While in these former treatments the density at the sonic point and the density slope entered as crucial free parameters, to be determined somehow from the observations, our unified models yield the IR-excess selfconsistently without any further assumptions as to choose T_{eff}, log g, R_*.

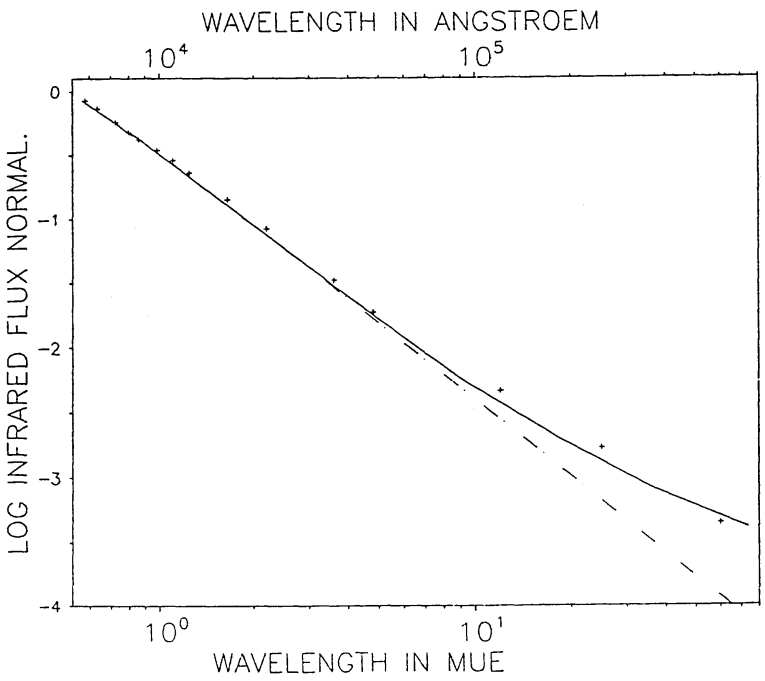

Fig. 7. IR energy distribution for ζ Puppis of the unified models (fully drawn) and the plane-parallel models (dash-dotted). The crosses represent the observations as given by Lamers et al.(1984)

The emergent line profiles of some strategic lines for the detailed NLTE photospheric analysis are shown in Fig.8. The He II Pickering lines λλ 5412, 4542, 4200 (transitions *n=4* to *n=7,9,11* respectively) show a decreasing degree of contamination by wind emission. λ 5412 is clearly wind affected, although it would be hard to detect this effect on the basis of observational data (see Bohannan et al., 1986, for the observed profile and hydrostatic calculations only). λ 4542 exhibits wind effects only in the very core, whereas λ 4200 is almost entirely photospheric (the difference in the wing is caused by a different treatment of higher levels in the hydrostatic case). We therefore conclude that no significant errors are introduced by the use of plane-parallel hydrostatic calculations for He II 4542 and 4200.

For the important hydrogen line H_γ, normally used for the gravity determination, this conclusion (as previously made by Kudritzki et al., 1983) would be incorrect. This line is filled by weak wind emission over the entire profile. Thus, this line simply appears a little weaker due to wind effects.

note For the gravity determination using hydrostatic models this means, that hydrostatic gravities are systematically a little too low for objects with strong winds, e.g. Of stars.

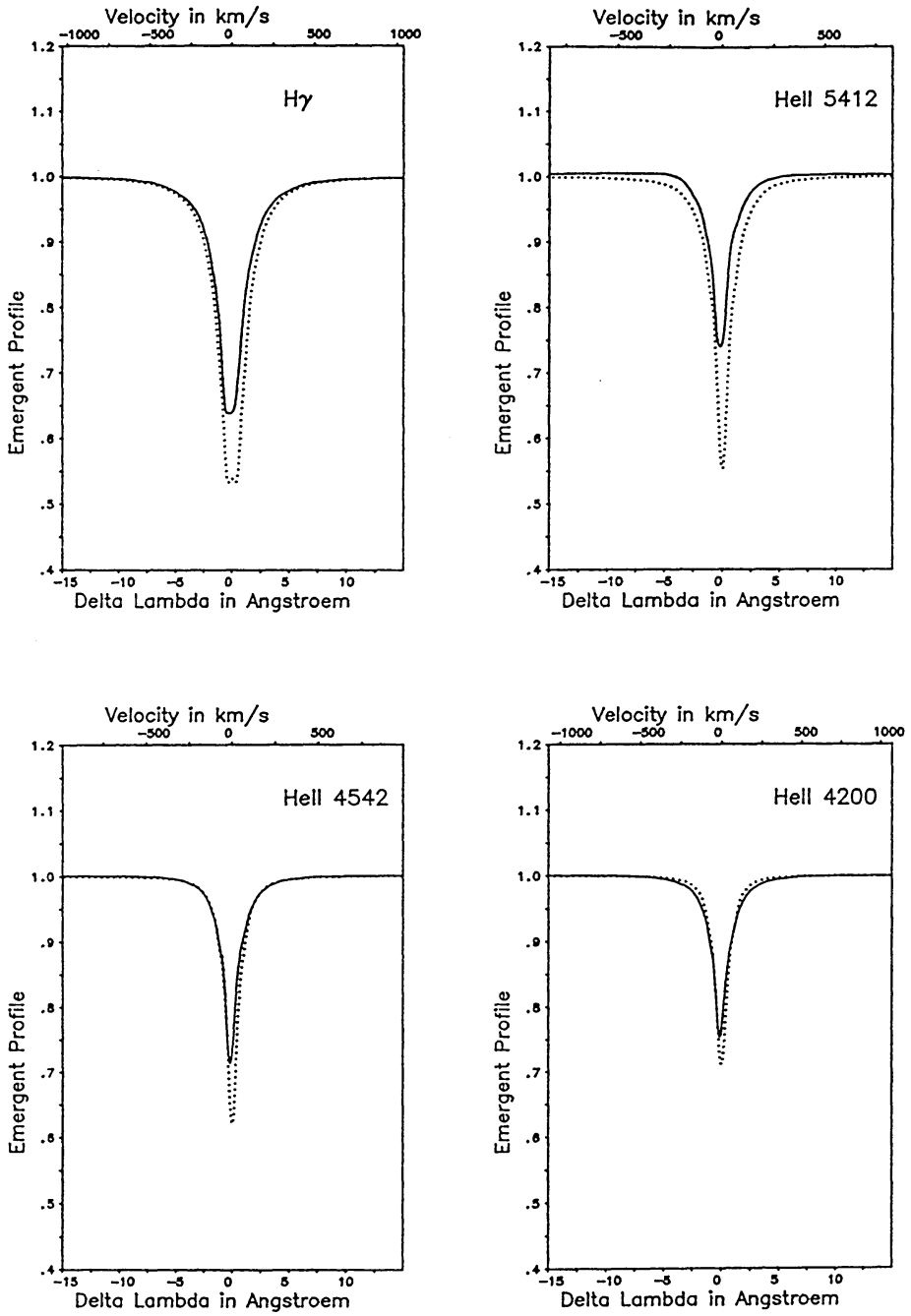

Fig. 8. Profiles of H_γ, He II 5412, 4542, 4200 of the comoving frame calculations (fully drawn) and hydrostatic plane-parallel models (dotted).

While the effects of wind contamination are extremely moderate for the "strategic NLTE analysis lines", clear effects are found for H_β,H_α,He II 4686 and He II 1640. This is demonstrated by the profiles given in Fig.9, where the large difference between the old hydrostatic and our new unified models is obvious.(In passing we note that He II 4686 roughly agrees with the observed profiles, whereas the H_α emission predicted by this unified model B is still too weak.)

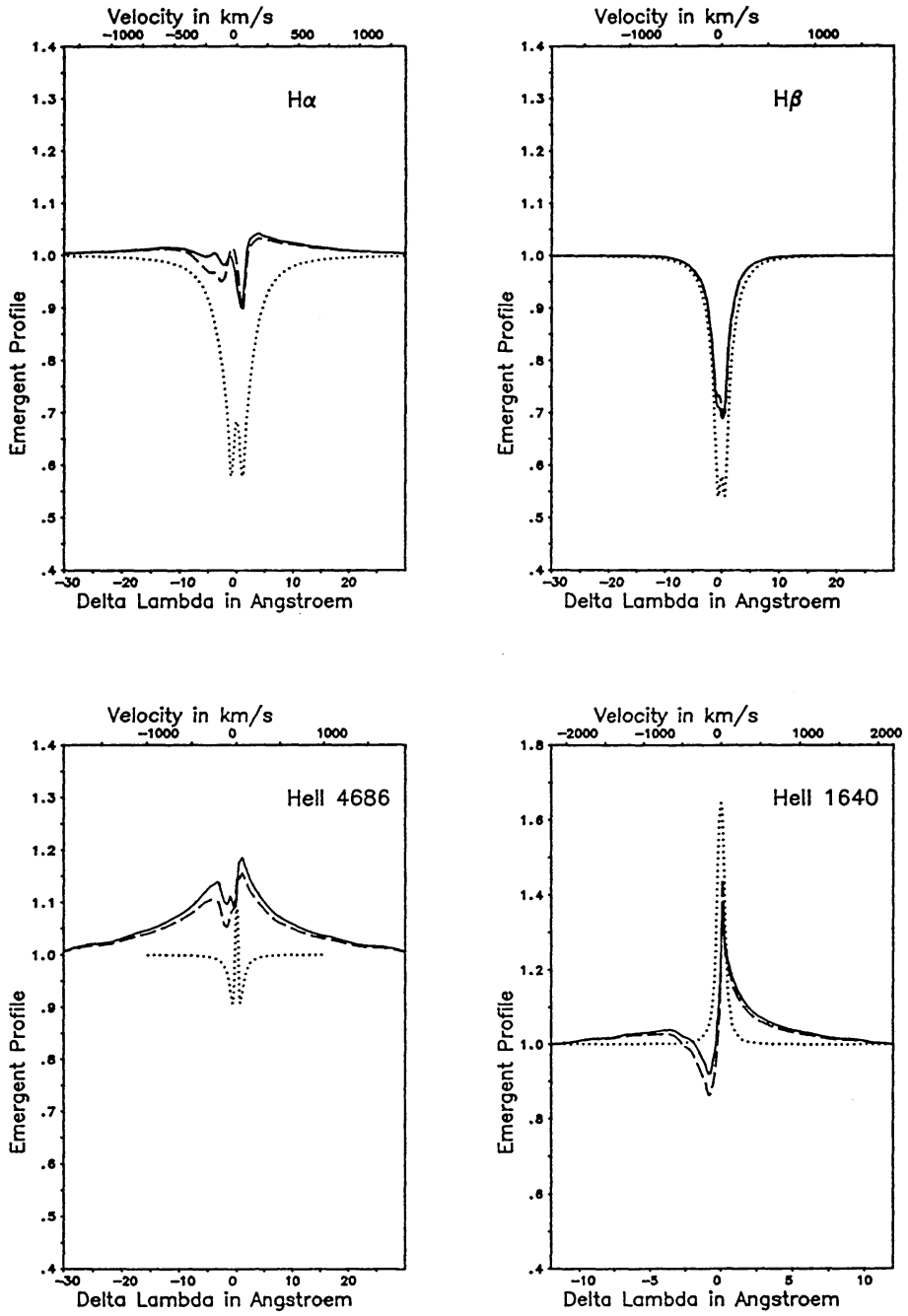

Fig. 9. Profiles of H_α,H_β,He II 4686 and He II 1640 of the unified models (dashed), subsequent comoving frame calculations (fully drawn) and hydrostatic plane-parallel models (dotted).

CONCLUSION

In spite of the remaining inconsistencies of the unified model:

— no metal opacities in the radiative equilibrium equation and the statistical equations (comes in only in the density structure i.e the stellar wind code),

— no iteration of the density structure after determination of the NLTE temperature structure (because of the deficient metal opacities, the wind temperature calculated from the unified model code has not the right value).

the results are encouraging:

— "photospheric lines normally used for the quantitative NLTE analysis of O stars, remain unaffected by sphericity and winds and are reproduced from the unified models as well as the typical wind lines and the infrared excess,

— due to the He II ground state formation problem, unified models predict orders of magnitude more photons in the spectral region of $\lambda < 228$ Å than the conventional plane-parallel NLTE models do.

Acknowledgements. This work was supported within the DFG-Schwerpunkt "Theorie kosmischer Plasmen" under grants Ku 474-11/2 and Ku 474-13/1/2.

REFERENCES

Abbott, D.C., Hummer, D.G.: 1985, *Astrophys. J.* **294**, 286
Anderson, L.S.: 1985, *Astrophys. J.* **298**, 848
Auer, L.H., Mihalas, D.: 1972, *Astrophys. J. Suppl.* **185**, 641
Bohannan, B., Abbott, D.C., Voels, S.A., Hummer, D.G.: 1986, *Astrophys. J.* **308**, 728
Castor, R.I., Simon, T.: 1983, *Astrophys. J.* **265**, 304
Drew, J.: 1988, *preprint*
Gruschinske, J..Kudritzki, R.P.: 1979, *Astron. Astrophys.* **77**, 341
Husfeld, D., Kudritzki, R.P., Simon, K.P., Clegg, R.E.S.: 1984, *Astron. Astrophys.* **134**, 139
Kudritzki, R.P.: 1979, *Common. of 22nd Intern. Liege Astrophys. Coll.*, p.295
Kudritzki, R.P., Simon, K.P., Hamann, W.R.: 1983, *Astron. Astrophys.* **118**, 245
Lamers, H.J.G.L.M., Waters, L.B.F.M.: 1984, *Astron. Astrophys.* **136**, 37
Lamers, H.J.G.L.M., Waters, L.B.F.M. Wesselius, P.R.: 1984, *Astron. Astrophys.* **134**, L17
Mihalas, D.: 1972, *Non-LTE Model Atmospheres for B and O stars*, NCAR-TN/STR-76
Mihalas, D., Hummer, D.G.: 1974, *Astophys. J. Suppl.* **265**, 343
Panagia, N., Felli, M.: 1975, *Astron. Astrophys.* **39**, 1
Pauldrach, A.W.A.: 1987a, Thesis, Ludwig-Maximilians-Universität, München
Pauldrach, A.W.A.: 1987b, *Astron. Astrophys.* **164**, 86
Pauldrach, A.W.A., Puls, J., Kudritzki, R.P.: 1986, *Astron. Astrophys.* **164**, 86
Pauldrach, A.W.A., Herrero, A.: 1988, *Astron. Astrophys.* **199**, 262
Werner, K.: 1988, *Astron. Astrophys.* **204**, 159
Werner, K., Husfeld, D.: 1985, *Astron. Astrophys.* **148**, 417
Wright, A.E., Barlow, M.J.: 1975, *Monthly Notices Roy. Astron. Soc.* **170**, 41